

## Short Note

# An immersed boundary method for restricted diffusion with permeable interfaces

Huaxiong Huang<sup>a,\*</sup>, Kazuyasu Sugiyama<sup>b</sup>, Shu Takagi<sup>b,c</sup>

<sup>a</sup> Department of Mathematics and Statistics, York University, Toronto, Ontario, Canada M3J 1P3

<sup>b</sup> Department of Mechanical Engineering, The University of Tokyo, 7-3-1 Hongo, Bunkyo-ku, Tokyo 113-8656, Japan

<sup>c</sup> Riken Institute, 2-1Hirosawa, Wako, Saitama, Japan

---

## ARTICLE INFO

### Article history:

Received 11 December 2008

Received in revised form 9 April 2009

Accepted 21 April 2009

Available online 7 May 2009

### Keywords:

Restricted diffusion

Permeable interface

Immersed boundary method

---

## 1. Introduction

In this note we present an immersed boundary (IB) method for restricted diffusion with permeable interfaces. These problems arise under a variety of circumstances, e.g., in thermal contact problems [7]. Diffusion in a medium consisting of two regimes separated by permeable boundaries is another example. It is well known that cell boundaries in a living tissue are permeable to oxygen and water molecules [3]. In this case, the cell boundaries can be treated as interfaces permeable to diffusive fluxes.

Typically, the conduction of heat and diffusive motion of molecules can be described by the diffusion equation in the bulk

$$c_t = \nabla \cdot (D\nabla c), \quad (1)$$

where  $c$  is the concentration (or temperature) and  $D$  is the diffusion coefficient. At the interface  $\Gamma$ , a flux law is also needed and given in this note in a relatively general form<sup>1</sup>

$$D\nabla c = P[g(c)]_r \mathbf{n} \quad (2)$$

for a given function  $g$ . Here  $P$  is the permeability,  $[\cdot]_r$  denotes the jump of concentration across the interface and  $\mathbf{n}$  is the unit normal vector of the interface. Standard numerical methods such as the finite difference or finite element methods can be used to solve the above problem. In the context of finite difference/volume methods, one can either try to map the interface into a regular shape so that it coincides with the grid or use an unstructured grid. The finite element method is better equipped for this problem as the interface can be naturally approximated. However, it becomes less efficient when the interface moves.

---

\* Corresponding author.

E-mail addresses: [hhuang@yorku.ca](mailto:hhuang@yorku.ca), [hhuang@mathstat.yorku.ca](mailto:hhuang@mathstat.yorku.ca) (H. Huang), [sugiyama@fel.t.u-tokyo.ac.jp](mailto:sugiyama@fel.t.u-tokyo.ac.jp) (K. Sugiyama), [takagish@riken.jp](mailto:takagish@riken.jp) (S. Takagi).

<sup>1</sup> This interface condition implies that there is no flux in the tangential direction. It is an assumption made here to simplify the presentation.

The immersed boundary (IB) method is an elegant numerical technique developed by Peskin [9,10] to simulate the interaction between immersed elastic fibers with the carrying fluid, as a model for the pumping motion of a human heart. It has the advantage of solving a complicated moving interface problem on a fixed Cartesian grid by a standard finite difference (volume) method. The IB method, due to its simplicity, has been applied to many fluid flow problems and become one of the main numerical techniques for scientific computation [8,11]. A closely related method which has gained popularity in recent years is the immersed interface method developed in [6]. In the context of porous interfaces, a number of authors have developed models which incorporated porosity into the immersed boundary and immersed interface frameworks, cf. [1,4,5,12].

In this note, we propose an IB method for the restricted diffusion problem, as a first step toward developing an efficient numerical method for solving fluid–structure interaction [12] coupled with diffusion of solvents. The key idea of our method is to use flux as an additional variable  $\mathbf{f}$  (vector in the multidimensional case). Using both  $c$  and  $\mathbf{f}$ , we reformulate the original problem given by (1) and (2) into a single set of equations which are valid in the entire domain, including the bulk region and the interfaces, standard finite difference approximation can be applied on a uniform grid. Our method can be extended to problems in multiple space dimensions with moving interfaces. For simplicity, we will restrict our discussion for problems with fixed interfaces in this note and postpone the discussion on the moving interface problems in a future paper where both diffusion and convection are present.

## 2. IB formulation

To simplify the presentation and without loss of generality, we consider a domain  $\Omega$  with an immersed permeable interface  $\Gamma$ . The diffusion problem can be re-formulated under the immersed boundary framework by applying the following equation on the entire domain  $\Omega$

$$c_t = \nabla \cdot \left( D \nabla c + \int_{\Gamma} \frac{D \mathbf{f}}{Pg'(c)} \delta(\mathbf{x} - \mathbf{x}_r) d\mathbf{x}_r \right), \quad (3)$$

where  $\mathbf{f}$  is the flux and  $\delta(\mathbf{x} - \mathbf{x}_r)$  is the delta function. It is easy to see that (3) is equivalent to (1) when  $\mathbf{x} \in \Omega/\Gamma$ . The singular term forces a jump in  $c$  at the interface  $\Gamma$  and below we give a brief justification on how condition (2) leads to Eq. (3).

Since  $c$  is smooth everywhere except at the interface  $\Gamma$ , we write  $c = c^s + [c]H(\mathbf{x} - \mathbf{x}_r)$  where  $H$  takes the values of zero on one side of the interface and one on the other side. Taking the gradient yields

$$\nabla c = \nabla c^s + \mathbf{n} \int_{\Gamma} [c] \delta(\mathbf{x} - \mathbf{x}_r) d\mathbf{x}_r = \nabla c^s - \int_{\Gamma} \frac{\mathbf{f}}{Pg'(c)} \delta(\mathbf{x} - \mathbf{x}_r) d\mathbf{x}_r$$

using Eq. (2). Therefore,

$$D \nabla c + \int_{\Gamma} \frac{D \mathbf{f}}{Pg'(c)} \delta(\mathbf{x} - \mathbf{x}_r) d\mathbf{x}_r = D \nabla c^s$$

and

$$\nabla \cdot \left( D \nabla c + \int_{\Gamma} \frac{D \mathbf{f}}{Pg'(c)} \delta(\mathbf{x} - \mathbf{x}_r) d\mathbf{x}_r \right) = \nabla \cdot (D \nabla c^s).$$

When the flux is continuous, the jump  $[c]$  does not contribute to the flux, thus

$$\nabla \cdot (D \nabla c^s) = -\nabla \cdot \mathbf{f} = c_t.$$

In order to solve for  $c$  using (3), we need to find a way to compute the flux  $\mathbf{f}$  on the entire domain  $\Omega$ . First of all, we note that in  $\Omega/\Gamma$ , by applying the following identity:

$$\nabla(g'(c)c_t) = g'(c)(\nabla c)_t + g''(c)c_t \nabla c, \quad (4)$$

and Eq. (1), we obtain the following equation:

$$g'(c)\mathbf{f}_t = g''(c)\mathbf{f} \nabla \cdot \mathbf{f} + D \nabla(g'(c) \nabla \cdot \mathbf{f}). \quad (5)$$

On the other hand, by taking the time derivative of the jump condition (2), we obtain

$$\mathbf{f}_t \cdot \mathbf{n} = P[g'(c) \nabla \cdot \mathbf{f}]_{\Gamma}. \quad (6)$$

The equation for  $\mathbf{f}$  on the entire domain  $\Omega$  can be obtained by combining Eq. (5) with condition (2)

$$\mathbf{f}_t \left( g'(c) + \int_{\Gamma} \frac{D}{P} \delta(\mathbf{x} - \mathbf{x}_r) d\mathbf{x}_r \right) = g''(c)\mathbf{f} \nabla \cdot \mathbf{f} + D \nabla(g'(c) \nabla \cdot \mathbf{f}). \quad (7)$$

It is easy to verify that (7) implies (5) for  $\mathbf{x} \in \Omega/\Gamma$ . Furthermore, integrating (7) across the interface  $\Gamma$  yields the jump condition (6).

To solve (3) and (7) numerically, we replace the delta function by its discrete version,  $\delta_h$ , and discretize the equation using standard finite volume method. In this study, we use the following discrete delta function proposed by Peskin [9]

$$\delta_h = \frac{1}{(2h)^d} \prod_{j=1}^d \left( 1 + \cos \frac{\pi(x_j - x_{r,j})}{h} \right) \tag{8}$$

for  $|x_j - x_{r,j}| \leq h$  for  $j = 1, \dots, d$  and  $\delta_h = 0$  otherwise. Here  $d$  is the dimension and  $h$  is the regularization parameter, normally taken as the grid size.

### 3. Numerical tests

We now present numerical tests by applying the proposed IB method to several problems in one and two space dimensions. Since our main objective is to demonstrate the applicability of the methodology, we have not attempted to carry out detailed convergence analysis.

#### 3.1. Heat conduction in solids with thermal contact resistance at the interface

Our first test is on heat conduction in solids where the heat transfer between the bulk regimes is given by two different laws, for comparison purposes. The first one is the linear (Newton’s cooling) law in the form of

$$D\nabla c \cdot \mathbf{n} = P[c], \tag{9}$$

where  $D = k/\rho c_p$  and  $P = h/\rho c_p$ . Here  $k$ ,  $\rho$  and  $h$  are the conductivity, density and heat transfer coefficient. This fits our general formulation with  $g(c) = c$  and the concentration of the particles and its flux satisfy the following coupled equations:

$$c_t = \nabla \cdot \left( D\nabla c + \int_{\Gamma} \frac{D\mathbf{f}}{P} \delta(\mathbf{x} - \mathbf{x}_r) d\mathbf{x}_r \right), \tag{10}$$

$$\mathbf{f}_t \left( 1 + \int_{\Gamma} \frac{D}{P} \delta(\mathbf{x} - \mathbf{x}_r) d\mathbf{x}_r \right) = D\nabla(\nabla \cdot \mathbf{f}). \tag{11}$$

The second law is by radiation,

$$D\nabla c \cdot \mathbf{n} = P[c^4], \tag{12}$$

where  $P = \sigma/\rho c_p$  and  $\sigma$  is the Stefan–Boltzmann constant. This corresponds the case with  $g(c) = c^4$  and the governing equations are

$$c_t = \nabla \cdot \left( D\nabla c + \int_{\Gamma} \frac{D\mathbf{f}}{4c^3P} \delta(\mathbf{x} - \mathbf{x}_r) d\mathbf{x}_r \right), \tag{13}$$

$$\mathbf{f}_t \left( 4c^3 + \int_{\Gamma} \frac{D}{P} \delta(\mathbf{x} - \mathbf{x}_r) d\mathbf{x}_r \right) = 12c^2 \mathbf{f} \nabla \cdot \mathbf{f} + D\nabla(4c^3 \nabla \cdot \mathbf{f}). \tag{14}$$

In Fig. 1(a) and (b), we have plotted the steady state solution of a one-dimensional heat transfer problem where the temperature is fixed at the each end of the interval. The interfaces are located at  $x_1 = 7/18$  and  $x_2 = 11/18$  and value of  $P$  is taken as  $1/5$  and  $D = 1$ . For each case, the exact solution can be obtained as

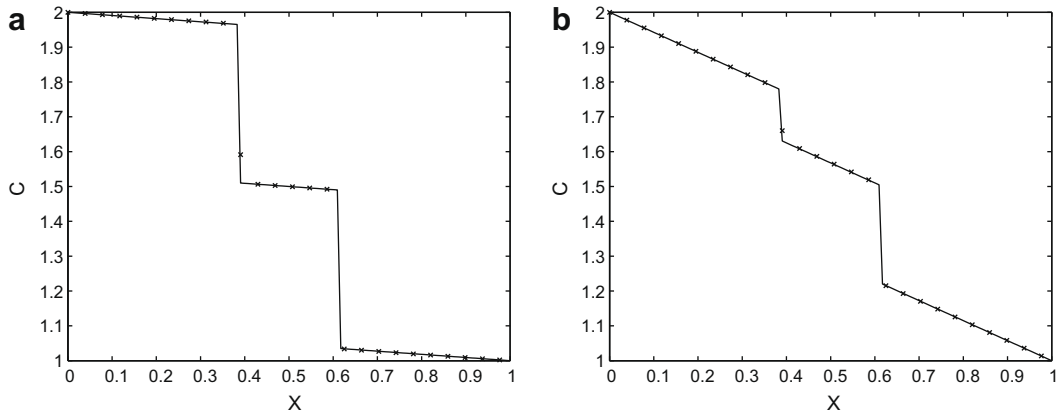


**Fig. 1.** Steady state solution with (a) the linear law and (b) nonlinear (radiation) law on the interfaces located at  $x_1 = 7/18$  and  $x_2 = 11/18$  with  $P = 0.2, D = 1, c_0 = 2$  and  $c_1 = 1$ . The solid lines are exact solutions and the symbols are numerical solutions computed on a grid with size  $\delta x = 0.02$ .

$$c = \begin{cases} mx + c_0, & x < x_1; \\ mx + c_m, & x_1 \leq x < x_2; \\ m(x - 1) + c_1, & x \geq x_2, \end{cases} \tag{15}$$

where  $c_0$  and  $c_1$  are the values of the solution at  $x = 0$  and  $1$ , respectively. For the linear flux law at the interface,  $m$  and  $c_m$  can be obtained as

$$m = \frac{c_1 - c_0}{2DP^{-1} + 1}, \quad c_m = \frac{DP^{-1}(c_0 + c_1) + c_0}{2DP^{-1} + 1}.$$

However, for the nonlinear fourth order law, we need to solve a set of two nonlinear equations given by the jump conditions at  $x_1$  and  $x_2$ . More in-depth discussions on thermal contact resistance can be found in [7].

### 3.2. Diffusion of non-ionic particles

We now present test results for the diffusion of non-ionic particles. We consider the case where the flux is linearly proportional to the jump of the concentration

$$D\nabla c \cdot \mathbf{n} = P[c]_I. \tag{16}$$

#### 3.2.1. An one-dimensional example

In Fig. 2(a), we have plotted the evolution of the concentration in one space dimension, starting from initial condition  $c(t_0, x) = G(t_0, x - x_0)$  where

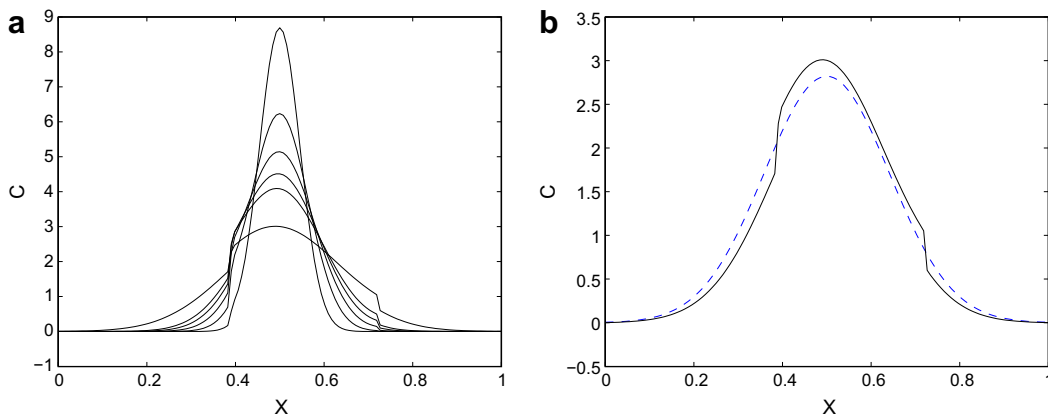


**Fig. 2.** Evolution of concentration from initial condition  $c(t_0, x) = G(t_0, x - x_0)$  where  $t_0 = 10^{-4}$  and  $G(t, x)$  is the fundamental solution, (a) at  $t - t_0 = 10^{-3}, 2 \times 10^{-3}, 3 \times 10^{-3}, 4 \times 10^{-3}, 5 \times 10^{-3}$  and  $10^{-2}$ ; (b) comparison between unrestricted (broken line) and restricted (solid line) diffusion at  $t = t_0 + 10^{-3}$ . The interfaces are located at  $x = 7/18$  and  $x = 13/18$  and the computations are done on a grid with size  $\delta x = 0.02$ .

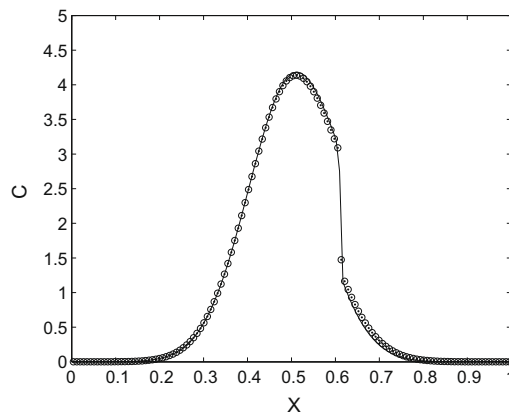


**Fig. 3.** Concentration at  $t = t_0 + 5 \times 10^{-3}$  with a flat interface located at  $x = 11/18$ . The initial solution is  $c(t_0, x, y) = G(t_0, x - x_0)$ . The solid line is the result from one-dimensional computation and the dots and circles are from two-dimensional computation, at  $y = 0$  and  $y = 0.5$ , respectively.

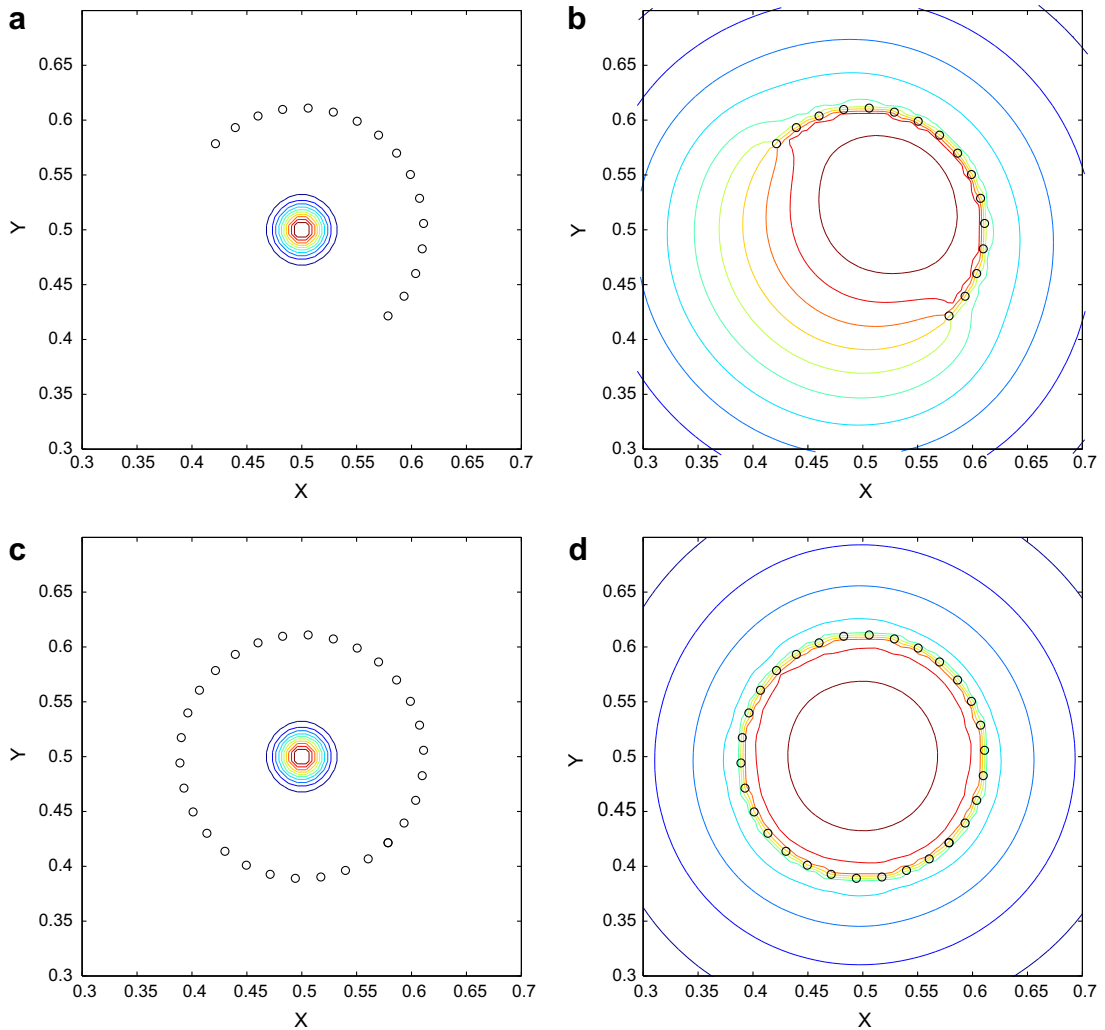


**Fig. 4.** Contours of concentration at time  $t = t_0 + 10^{-2}$ : (b) and (d) with semi-circular and circular interfaces, respectively. The corresponding initial solution  $c(t_0, x, y) = G_2(t_0, x - x_0, y - y_0)$  for  $t_0 = 10^{-4}$  are shown in (a) and (c). The circles indicate the marker points on the interface (not all are shown).

$$G(t, x) = \frac{1}{\sqrt{4\pi Dt}} e^{-\frac{x^2}{4Dt}}.$$

We have taken  $x_0 = 0.5$  and  $t_0 = 10^{-4}$  with two interfaces at  $x = 7/18$  and  $x = 13/18$ . The parameter values are  $D = 1$  and  $P = 50$ . In Fig. 2(b), we compare the values of the concentration at  $t = t_0 + 10^{-3}$  between the one with interfaces (solid line) and the one without interface (broken line),  $G(t, x - x_0)$ .

### 3.2.2. Two-dimensional examples

We have carried out two tests, one with flat interface and the other with an interface in the form of a circular arc. In the first test, we start the computation with an initial condition  $c(t_0, x, y) = G(t_0, x - x_0)$  and an interface at  $x = 11/18$ . The solution is one-dimensional and agrees well with the one-dimensional computation, cf. Fig. 3.

In the second example, we use initial condition  $c(t_0, x, y) = G_2(t_0, x - x_0, y - y_0)$  where

$$G_2(t, x, y) = \frac{1}{4\pi Dt} e^{-\frac{x^2 + y^2}{4Dt}}.$$

We considered two cases: one with a semi-circular interface and the other with a circular interface. The evolution of the concentration at  $t = t_0 = 10^{-4}$  and  $t = t_0 + 10^{-2}$  is shown in Fig. 4 for both cases.

All the computations are carried out on a uniform grid with size  $1/128$ . The marker points on the interface are 120 and 60 for the circular and semi-circular interfaces, respectively. The other parameters are chosen as  $D = 1$  and  $P = 10$ .

#### 4. Conclusion

In this note we have presented an immersed boundary method for restricted diffusion with permeable interfaces. We used diffusion in a domain with simple interfaces as examples to illustrate the basic idea. Our method is applicable to more general problems and work is underway to extend the method to convection–diffusion problems with more complex interface shapes. A related issue needs to be explored further is the stiffness of the IB formulation and its implication for time-stepping schemes. Analysis along the line of [13,2] will be of practical interest.

#### Acknowledgments

The authors wish to acknowledge the financial support from the Computational Science Research Program, Integrated Simulation of Living Matter by MEXT (Japan), Riken Institute (Japan), NSERC (Canada) and MITACS (Canada) and helpful discussions with R.M. Miura, X. Gong, S. Li, and P. Wilson.

#### References

- [1] K.M. Arthurs, L.C. Moore, C.S. Peskin, E.B. Pitman, H.E. Layton, Modeling arteriolar flow and mass transport using the immersed boundary method, *J. Comput. Phys.* 147 (1998) 402–440.
- [2] Z.X. Gong, H. Huang, C. Lu, Stability analysis of the immersed boundary method for a two-dimensional membrane with bending rigidity, *Commun. Comput. Phys.* 3 (2008) 704–723.
- [3] J. Keener, J. Sneyd, *Mathematical Physiology*, Springer-Verlag, NY, 1998.
- [4] Y. Kim, C.S. Peskin, 2-D parachute simulation by the immersed boundary method, *SIAM J. Sci. Comput.* 28 (6) (2006) 2294–2312.
- [5] A.T. Layton, Modeling water transport across elastic boundaries using an explicit jump method, *SIAM J. Sci. Comput.* 28 (6) (2006) 2189–2207.
- [6] R.J. LeVeque, Z. Li, The immersed interface method for elliptic equations with discontinuous coefficients and singular sources, *SIAM J. Numer. Anal.* 31 (1994) 1019–1044.
- [7] C.V. Madhusudana, *Thermal Contact Conductance*, Springer, 1996.
- [8] R. Mittal, Immersed boundary methods, *Ann. Rev. Fluid Mech.* 37 (2005) 239–261.
- [9] C.S. Peskin, *Flow Patterns Around Heart Valves*, Ph.D. Thesis, Albert Einstein College of Medicine, 1972.
- [10] C.S. Peskin, Flow patterns around heart valves: a numerical method, *J. Comput. Phys.* 10 (1972) 252–271.
- [11] C.S. Peskin, The immersed boundary method, *Acta Numer.* 11 (2002) 479–518.
- [12] J.M. Stockie, Modelling and simulation of porous immersed boundaries, *Comput. Struct.*, in press, doi:10.1016/j.compstruc.2008.11.001.
- [13] J.M. Stockie, B.R. Wetton, Analysis of stiffness in the immersed boundary method and implications for time-stepping schemes, *J. Comput. Phys.* 154 (1999) 41–64.